GRAPPA-based simultaneous multislice reconstruction using concentric ring k-space

Alan Chu[1] and Douglas C. Noll[1]
[1]*Biomedical Engineering, University of Michigan, Ann Arbor, MI, United States*

PURPOSE: Simultaneous multislice (SMS) imaging is an effective method for accelerating fMRI and DTI because it can provide acceleration even with the single-shot acquisitions commonly used in these applications. Previous SMS methods have either focused on Cartesian trajectories [1], or used time-consuming iterative SENSE-like reconstructions on spiral data [2]. We propose a non-iterative GRAPPA-based reconstruction method on non-Cartesian data. A concentric ring trajectory is used to facilitate the sampling regularity needed for accurate kernel weights, and a blipped z-gradient is used to help slice separation [1,2]. The concentric ring trajectory achieves most of the same benefits as conventional spirals in fMRI, with only a small increase in readout length. The methods and results here use 3 simultaneous slices with an 8-channel head coil.

METHODS: A concentric rings k_x-k_y trajectory, shown in Figure 1, was developed using a numerical algorithm inspired by Pipe et al [3]. The numerical algorithm consecutively samples a concentric circle in k-space, using the maximum gradient slew rate allowed by the scanner at every step to achieve the fastest possible sampling. When the curvature of the trajectory is too great for the slew rate limit, the algorithm backs up to a previous sample, and re-samples the trajectory so that the samples are closer together, equivalent to "slowing down" the trajectory. This allows for fast sampling that still respects hardware limits. The transitions between concentric rings were designed to accommodate the length of the readout z-gradient blips so that entire circle revolutions occur in each of the 3 platters shown in Figure 1. This way, the transition samples can be thrown out and spiral GRAPPA can be applied to only the concentric rings in each platter, each of which are perfectly 3x undersampled.

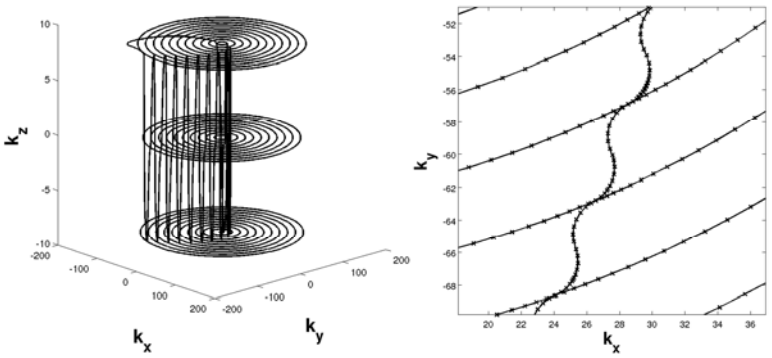

Fig 1: Left: Full 3D concentric ring trajectory with z-gradient blipping. Right: Close-up of transition samples.

For reconstruction, a non-Cartesian GRAPPA method based on [1] and [4] was used. A non-SMS volume was acquired with the same z-gradient readout modulation as the SMS scans, and with matching slice locations. In addition, an SMS volume was acquired (with z-gradient modulation) using the same TR as the non-SMS volume and with a similar flip angle in order to match image contrast as much as possible. These 2 volumes were used to calibrate the GRAPPA weights used for slice separation. First, the concentric ring sampling of both the non-SMS and SMS volumes are linearly interpolated to constant angular velocity trajectories. These constant angular velocity trajectories are then "unwound" to form a Cartesian grid. This Cartesian grid is then divided into 2 radial sectors, each of which is divided into 8 angular sectors. Slice-GRAPPA [1] is then performed on each of the sectors, where each sector has a different set of kernel weights. The kernel weights are then used to reconstruct all further repetitions of SMS scans, which may be acquired with a different (shorter) TR than with the calibration scans. After reconstruction of each SMS scan, the resulting slice-separated k-space data for all sectors is reassembled together using a linear smoothing across the sector boundaries. Next, the assembled, slice-separated k-space data is demodulated using the conjugate of the phase modulation resulting from the readout z-gradient. Finally, the k-space data is transformed back into the image domain using a gridding and IFFT procedure with conjugate phase inhomogeneity correction [5], and coil data is combined using the square-root-sum-of-squares.

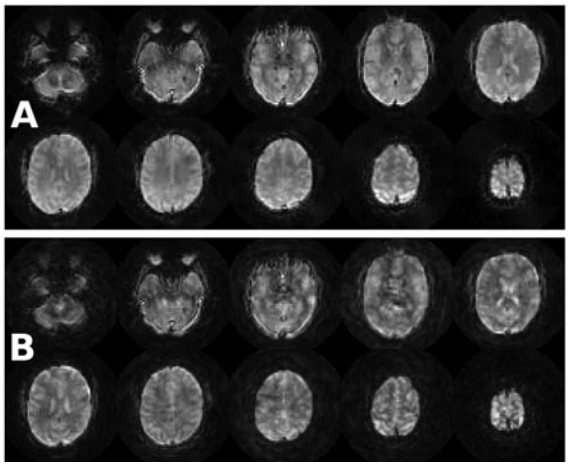

Fig 2: Human subject. A: non-SMS. B: SMS.

To demonstrate and evaluate the method, both an SMS scan and a non-SMS scan were performed on a subject using an 8-channel head coil. Both scans used the previously described concentric rings trajectory. Each SMS acquisition consisted of three simultaneous 3 mm thick slices, excited by an RF pulse consisting of 3 Hamming-weighted sincs, each of which was modulated in frequency to create a 13-slice gap between the simultaneous slices. Thirteen of these simultaneous slices were acquired per TR, resulting in 39 slices total. The non-SMS scan consisted of 39 separately excited slices at locations matching those of the SMS scan. The SMS scan used TE=30 ms and TR=667 ms, and the non-SMS scan used TE=30 ms and TR=2001 ms. The blipped readout z-gradient was designed according to principles described in [2]. The 2 calibration scans, described previously, were both acquired using TE=30 ms, TR=2001 ms, and a flip angle of 30 degrees. Reconstructed images are shown in Figure 2.

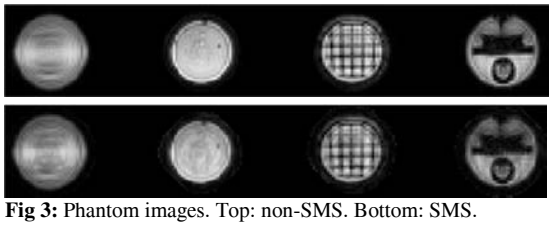

Fig 3: Phantom images. Top: non-SMS. Bottom: SMS.

RESULTS: Reconstructed images comparing non-SMS and SMS acquisitions are shown in Figures 2 and 3, demonstrating good separation of the slices with only a slight increase in noise-like structure due to unsuppressed slice-aliasing.

CONCLUSION: A non-iterative GRAPPA-based reconstruction algorithm for non-Cartesian data was presented. This method potentially reduces the time needed for image reconstruction relative to non-Cartesian SENSE SMS; once the weights have been computed, they can be used to very quickly reconstruct any number of SMS repetitions. Although preliminary results for the SMS scan show some artifacts, further refinements regarding the number of radial and angular sectors, kernel size, and training regions can potentially improve the images. Point-spread-function analysis of the reconstruction framework can be used to determine the optimal reconstruction parameters. Future work will involve performing fMRI scans to compare the effect of increased temporal resolution with regard to physiological noise reduction, and noise and slice-leakage analysis on the reconstruction process.

REFERENCES: [1] Setsompop et al. 2012. Magn Reson Med. 67:1210. [2] Zahneisen et al. 2013. Magn Reson Med. doi:10.1002/mrm.24875. [3] Pipe et al. 2013. Magn Reson Med. doi:10.1002/mrm.24675. [4] Heidemann et al. 2006. Magn Reson Med. 56:317. [5] Noll et al. 1991. IEEE TMI 10(4):629.